Biophysical *Journal*
Article

Biophysical Society

Modulation of *Escherichia coli* UvrD Single-Stranded DNA Translocation by DNA Base Composition

Eric J. Tomko[1] and Timothy M. Lohman[1,*]
[1]Department of Biochemistry and Molecular Biophysics, Washington University School of Medicine, St. Louis, Missouri

ABSTRACT *Escherichia coli* UvrD is an SF1A DNA helicase/translocase that functions in chromosomal DNA repair and replication of some plasmids. UvrD can also displace proteins such as RecA from DNA in its capacity as an anti-recombinase. Central to all of these activities is its ATP-driven 3′–5′ single-stranded (ss) DNA translocation activity. Previous ensemble transient kinetic studies have estimated the average translocation rate of a UvrD monomer on ssDNA composed solely of deoxythymidylates. Here we show that the rate of UvrD monomer translocation along ssDNA is influenced by DNA base composition, with UvrD having the fastest rate along polypyrimidines although decreasing nearly twofold on ssDNA containing equal amounts of the four bases. Experiments with DNA containing abasic sites and polyethylene glycol spacers show that the ssDNA base also influences translocation processivity. These results indicate that changes in base composition and backbone insertions influence the translocation rates, with increased ssDNA base stacking correlated with decreased translocation rates, supporting the proposal that base-stacking interactions are involved in the translocation mechanism.

INTRODUCTION

Escherichia coli UvrD is an SF1A DNA helicase (1–8) that translocates along single-stranded (ss) DNA with 3′–5′ directionality (9–11) and can catalyze the unwinding of duplex DNA to produce the ssDNA intermediates required for methyl-directed mismatch repair (12) and nucleotide excision repair (13). *E. coli* UvrD also is involved in replication restart (14–16) and plasmid replication (17). UvrD monomers can rapidly and processively translocate along ssDNA in an ATP-dependent manner (6,9,10,18,19), although the monomer has no detectable helicase activity in vitro (6,9,11,20), unless tension is applied to the DNA (21). In fact, UvrD must self-assemble to form at least a dimeric complex to activate its processive helicase activity in vitro (6,11,20,22). In addition to its helicase activity, UvrD facilitates displacement of RecA protein filaments on ssDNA, presumably by utilizing its ssDNA translocase activity (23,24). UvrD can also push *E. coli* single-stranded DNA binding protein along ssDNA (25) and alter RNAP transcription elongation complexes blocked by DNA damage by working in conjunction with DinG and Rep to displace RNAP from the DNA ahead of a stalled replisome (26,27) or by pulling RNAP into a back-tracked state to expose damaged DNA to DNA repair enzymes (28).

Because ssDNA translocation is central to all activities of UvrD, it is important to understand the role of translocation in the more complex processes of DNA unwinding and protein displacement. Theoretical models of DNA unwinding predict that the ratio of the DNA unwinding rate to ssDNA translocation rate can indicate whether the helicase unwinds DNA using a passive mechanism in which the helicase stabilizes ssDNA upon thermal fraying of the double-stranded (ds) DNA end, or an active mechanism in which the helicase plays a direct role in dsDNA melting (29–32). DNA unwinding and ssDNA translocation rates have been determined for a number of DNA helicases (RecBCD (33,34), RecBC (35,36), PcrA (37), RepΔ2B (38), Dda (39), and UvrD (6,9)), under identical solution conditions; however, the ssDNA translocation studies have generally used ssDNA substrates comprised solely of oligodeoxythymidylates (oligo dT) to avoid internal basepairing. Furthermore, for Rep, UvrD, and PcrA, the active oligomeric forms of the helicase (dimers) are different from the ssDNA translocases (monomers) (40).

The effect of ssDNA base composition on the ssDNA translocation rate has been studied for only a few translocating

Submitted July 12, 2017, and accepted for publication August 16, 2017.
*Correspondence: lohman@biochem.wustl.edu
Editor: Enrique De La Cruz.
http://dx.doi.org/10.1016/j.bpj.2017.08.023

motors. These earlier studies showed an effect of ssDNA base composition on ssDNA translocation (41,42), as inferred from changes in the observed steady-state ATP hydrolysis rate. In some cases, the translocation rate varied a fewfold with faster translocation observed along pyrimidines than along purines. Studies with the SF1 DNA helicase PcrA from *Bacillus stearothermophilus* have yielded mixed results where no effect on ssDNA translocation was reported on a short oligodeoxynucleotide of mixed base composition when translocation was monitored indirectly via pre-steady-state ATP hydrolysis (43), whereas studies using a fluorescently labeled PcrA inferred base composition-dependent translocation rates (44). Recently, a study of the ss nucleic acid (ssNA) translocation kinetics of the SF2A NS3h helicase of Hepatitis C virus showed a large effect of translocation rate on base and sugar composition (45). Here we show that the ssDNA translocation rate and processivity of *E. coli* UvrD monomer are affected by ssDNA base composition. Our findings indicate that ssDNA base composition needs to be considered when comparing ssDNA translocation and DNA unwinding rates and that base-stacking interactions play a central role in the UvrD translocation mechanism.

MATERIALS AND METHODS

Buffers and reagents

Buffers were prepared with reagent grade chemicals using distilled water, further deionized with a Milli-Q purification system (Millipore, Bedford, MA), and then filtered through 0.2 μm filters. Buffer T_{20} is 10 mM Tris-HCl (pH 8.3 at 25°C), 20 mM NaCl, and 20% (v/v) glycerol (enzyme grade). Other buffers are described in Supporting Material.

Enzymes and DNA

E. coli UvrD was purified and its concentration determined as described (5) and was stored at −20°C in minimal storage buffer for up to six months without loss of translocation activity. The ssDNA substrates used to construct the 5′-ss/dsDNA junction were labeled with fluorescein during synthesis, purified, dialyzed versus 10 mM Tris-HCl, pH 8.3, then stored at –20°C, and concentrations determined spectrophotometrically as previously described (9). Purified DNA substrates migrated as single species on a native PAGE gel. The base composition and annealing of the 5′-ss/dsDNA junction substrates is described in Supporting Material.

Stopped-flow experiments

Experiments were performed in buffer T_{20} at 25°C using an SX18MV stopped-flow (Applied Photophysics, Leatherhead, UK) as described (18). In translocation experiments, UvrD was preincubated with DNA in one syringe and reactions initiated by 1:1 mixing with buffer T_{20} plus 0.5 mM ATP, 2 mM $MgCl_2$, and 4 mg/mL heparin. All concentrations given are the final concentrations after mixing in the stopped-flow. UvrD monomer translocation kinetics were measured under single-round conditions (no rebinding of UvrD to ssDNA) using a fluorescent stopped-flow assay to monitor the arrival of UvrD at the 5′-end of the ssDNA region of the DNA substrates, which were labeled with fluorescein as described (18). UvrD monomer dissociation kinetics during translocation along 5′-ss/dsDNA substrates were monitored by the increase in UvrD tryptophan fluorescence as described (18).

Analysis of translocation time courses

As shown previously (18,46), if a translocase initiates at a unique site, the translocation rates along the variable region of ssDNA can be estimated by measuring the time to reach the minimum in the fluorescence time courses, referred to as the "time to trough", for a series of DNA molecules differing in ssDNA length, as follows (see Fig. 3 *A*). The time to trough (t^{obs}_{trough}) is the average time for UvrD to translocate from the ss/dsDNA junction to the fluorescein label at the 5′-end. This can be decomposed into the average time to translocate along the stretch of $(dT)_L$ ssDNA and ssDNA of variable base composition (dvr) ($t^{obs}_{trough}(s) = t_{dT}(s) + t_{dvr}(s) = (L_{dT}(nts)/k_t^{dT}(nts/s)) + (L_{dvr}(nts)/k_t^{dvr}(nts/s))$). Because we know the translocation rate along a stretch of dT ($k_t^{dT} = 191$ nts/s) (9,10,18) and the length (L) of the dT regions, we can determine the time it takes to translocate along the ssDNA of variable composition as ($t_{dvr}(s) = t^{obs}_{trough}(s) - (L_{dT}(nts)/k_t^{dT}(nts/s))$). A plot of $t_{dvr}(s)$ versus the length of variable composition ssDNA will be linear with a zero y intercept ($t_{dvr}(s) = (L_{dvr}(nts)/k_t^{dvr}(nts/s))$), with the inverse of the slope yielding the average translocation rate along the variable composition ssDNA. An estimate of the average translocation rate can also be determined from a single length of variable composition ssDNA by dividing the length of dvr by $t_{dvr}(s)$ ($k_t^{dvr(single\ L)} = L_{dvr}(nts)/t_{dvr}(s)$).

The percentage of UvrD reaching the 5′-end was estimated from the ratio of the total area under the translocation curve for a given 5′-F-ss/dsDNA containing variable base composition, abasic, or PEG modification to the total area under the translocation curve for the appropriate control 5′-F-ss/dsDNA substrate containing only $(dT)_L$.

RESULTS

Experimental approach and DNA substrate design

The translocation kinetics of a nucleic acid motor can be examined using ensemble stopped-flow approaches by monitoring the fluorescence change of a fluorophore covalently attached to one end of a nucleic acid (NA) (9,33,36,45–50), as depicted in Fig. 1 *A*. The ssNA is labeled covalently at one end with a fluorophore that undergoes a change in fluorescence intensity when the enzyme arrives at the fluorophore. A molar excess of DNA over the translocase is used to ensure no more than one translocase is bound to a NA. Because UvrD binds nonspecifically to the ssNA, it will initially bind randomly along the ssNA. Upon addition of ATP, the translocase moves with biased directionality (3′–5′ for UvrD) along the ssNA. When the translocase reaches the fluorophore at the end of the ssNA, the fluorophore fluorescence is enhanced or quenched. A trap for free enzyme (e.g., heparin) is added with ATP so that the enzyme that dissociates from the NA is prevented from rebinding, resulting in kinetic time courses reflecting a single round of translocation along the ssNA.

Because UvrD undergoes 3′–5′ directional translocation, we designed a series of ssDNA of varying length, L, labeled at the 5′ end with fluorescein, the fluorescence of which is quenched when UvrD monomer reaches it as

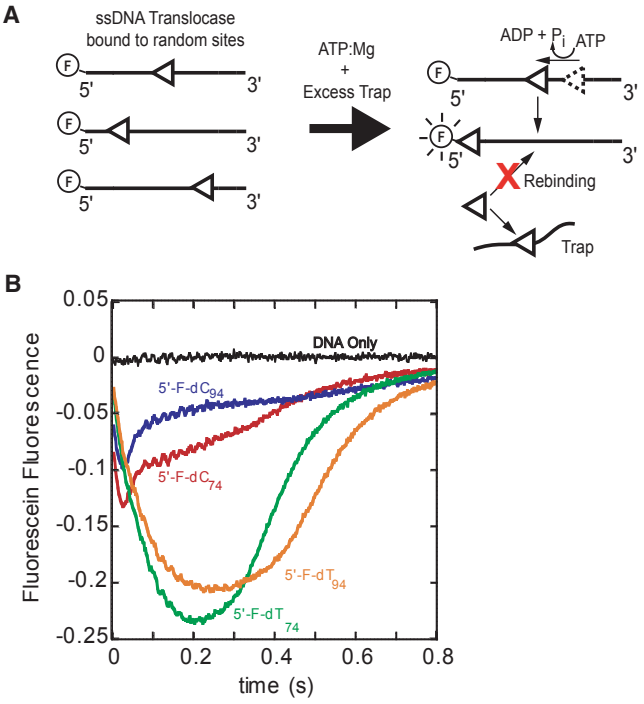

FIGURE 1 UvrD translocation time courses along ssDNA homopolydeoxynucleotides. (*A*) Depiction of the ssDNA translocation assay is given. UvrD (*triangle*) binds nonspecifically and randomly along the ssDNA. In a reaction coupled to ATP binding and hydrolysis, UvrD translocates along the ssDNA in a 3′–5′ direction. As UvrD reaches the 5′-end, it quenches the fluorescein fluorescence. Any UvrD that dissociates from the ssDNA is rapidly bound by a trap (heparin) that prevents rebinding to the ssDNA. (*B*) Given here are stopped-flow time courses monitoring fluorescein fluorescence during UvrD monomer translocation along two different lengths of either oligodeoxythymidylates or oligodeoxycytidylates. To see this figure in color, go online.

depicted in Fig. 1 *B* (9,10). To investigate the effect of base composition on translocation, we initially used ssDNA homo-oligodeoxynucleotides composed of a single base (e.g., oligodeoxycytidylate). However, with 5′-fluorescein (F)-labeled $(dC)_L$, we observed qualitatively different time courses than with 5′-F-$(dT)_L$ (Fig. 1 *B*). Furthermore, the simple *n*-step sequential model (51) that provides an excellent description of the time courses for UvrD translocation along 5′-F-$(dT)_L$ (9,10) does not adequately describe the time courses with 5′-F-$(dC)_L$. This could result from several causes, including the possibility that UvrD shows a preference for binding to either end of the $(dC)_L$ or that the interaction of UvrD with fluorescein attached to $(dC)_L$ is significantly different.

To circumvent these complications, we made two changes to our DNA substrates (Fig. 2 *A*): 1) we placed a ss/dsDNA partial duplex (-dT_{25}-DP_{18}) at the 3′-end, and 2) we added a 15-nt dT region at the fluorescein-labeled 5′-end. We have shown previously that UvrD monomers have high specificity for binding to 5′-ss/dsDNA junctions and will translocate away from the junction (in a 3′–5′ direction) along the 5′-ssDNA tail (18) as depicted schematically (Fig. 2 *B*). This modification results in a significant fraction of UvrD being initially bound at the 5′-ss/dsDNA junction, which simplifies determination of the translocation rate as discussed below. By placing regions of oligo dT at the 5′-end and the ss/dsDNA junction, we maintain the same interactions of UvrD with the ss/dsDNA junction and the 5′-end, avoiding any fluorophore-specific ssDNA base interactions. We then systematically varied the base composition of an internal portion of the 5′-ssDNA tail as depicted in Fig. 2 *A*.

UvrD monomer translocation along ssDNA possessing a 5′-ss/dsDNA partial duplex displays a characteristic time course that reflects the preference of UvrD to bind at the ss/dsDNA junction (17–20-fold higher specificity for junction than ssDNA) (18). The time course results from two populations of UvrD translocating with the same rate, but initially bound to the DNA substrate either randomly along the ssDNA tail or specifically at the ss/dsDNA junction (18). To illustrate this, we show simulated translocation time courses for three cases. Fig. 2 *C* shows translocation time courses for the case in which the DNA molecules have UvrD initially bound randomly to the ssDNA tails. Fig. 2 *D* shows translocation time courses for the case in which all UvrD is initially bound to the ss/dsDNA junction, and Fig. 2 *E* shows translocation time courses for the case in which there is a mixture of random UvrD binding to the ssDNA tail and UvrD binding to the ss/dsDNA junction. All three simulated time courses for each case change with ssDNA length, indicating that one can estimate rates of ssDNA translocation from these time courses as described previously (9,18,46,48,51,52). The simulated time courses in Fig. 2 *E* are a superposition of the time courses shown in Fig. 2, *C* and *D*, and thus show two phases. For the cases in which either all or some of the UvrD initiate at a unique site (Fig. 2, *D* and *E*), in this case the ss/ds DNA junction, we have shown that one can obtain an accurate estimate of the ssDNA translocation rate by determining the time to reach the trough of the fluorescence change for a series of DNA molecules differing in ssDNA length (18,46).

The experimental time courses show two phases similar to the simulations shown in Fig. 2 *E*. The initial phase (*shaded gray*, Fig. 3 *A*) reflects translocation to the 5′ labeled fluorescein by UvrD that was initially bound randomly along the ssDNA tail, whereas the second phase (*boxed region*, Fig. 3 *A*) reflects translocation to the 5′ labeled fluorescein by UvrD that initiated at the ss/dsDNA junction. A semiquantitative time-to-trough analysis in which the time to reach the minimum in the fluorescence signal, the trough, is plotted as a function of 5′-ssDNA-tail length (Fig. 3, *C* and *D*), can be used to determine the average translocation rate of UvrD initially bound at the ss/dsDNA junction (46). The time-to-trough is the average time for the UvrD population initially bound at the ss/dsDNA

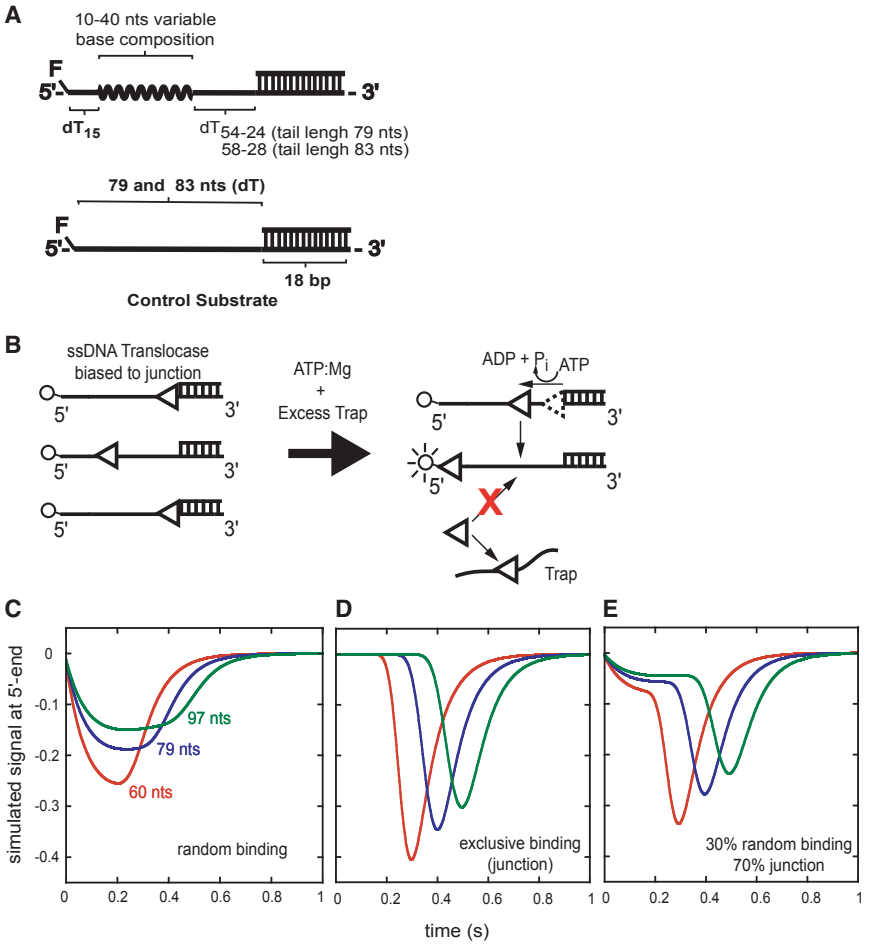

FIGURE 2 DNA substrate design and UvrD translocation on 5′ss/dsDNA partial duplex substrate. (*A*) 5′-ss/dsDNA partial duplex DNA substrates are given. (*B*) Given here is a depiction of ssDNA translocation assay using partial duplex DNA substrates and semiquantitative approach for determining translocation rate and fraction of UvrD reaching the 5′-end. UvrD (*triangle*) binds with limited specificity to the ss/dsDNA junction. Upon binding and hydrolyzing ATP, UvrD translocates along the ssDNA. When UvrD reaches the 5′-end, the fluorescein fluorescence is quenched. Any UvrD that dissociates from the ssDNA is rapidly bound to a protein trap (heparin), preventing rebinding to the ssDNA. (*C–E*). Shown here are simulated time courses for UvrD translocation to the 5′ end of ssDNA (labeled with fluorescein) for three ssDNA lengths as indicated when the UvrD population is initially bound (*C*) at random positions along the ssDNA, (*D*) UvrD is bound exclusively at the ss/dsDNA junction, and (*E*) the bound UvrD population initially exists bound both randomly to ssDNA and at the ss/dsDNA junction. For each simulation, the translocation rate was constrained to 191 nts/s, dissociation rate from internal sites is 0.8 s^{-1}, and dissociation from 5′-end is 12 s^{-1} (18). To see this figure in color, go online.

junctions to translocate the entire length of the ssDNA tail. From this one can readily determine the rate of translocation given the length of the ssDNA tail (nucleotides (nts)) (Fig. 3 *A*). Furthermore, for different lengths of ssDNA tails of the same base composition, the time-to-trough will increase linearly with ssDNA length such that the inverse of the slope of a plot of time-to-trough versus ssDNA length is equal to the average translocation rate (nts/s) (Fig. 3, *C* and *D*). Thus, on 5′-ss/dsDNA substrates with different ssDNA base composition, any effect of base composition can be readily determined as a change in the time-to-trough relative to the time-to-trough of a control DNA substrate containing only $(dT)_L$.

Our substrate design also enables a qualitative determination of translocation processivity to be assessed from the total area under the translocation signal (Fig. 3 *B*), because the area is directly proportional to the amount of UvrD that reaches the 5′-end (9). By maintaining a constant dT base composition at the 5′-end, UvrD dissociation from the 5′-end should remain the same regardless of changes in base composition at an internal region of the ssDNA tail. Thus, changes in the total area under the translocation signal for substrates with different base composition relative to the control substrate will reflect the relative amounts of UvrD that reach the 5′-end.

UvrD translocation along pyrimidines is faster than along ssDNA containing purines

The UvrD translocation rate along ssDNA comprised of deoxythymidylates is 191 ± 10 nts/s (T_{20} buffer, 0.5 mM ATP, 2.0 mM $MgCl_2$, and 4 mg/mL heparin at 25°C; Fig. 3 *D*) (10). To examine the effects of ssDNA base composition, we varied the base composition over an internal 40 nt stretch of the 5′-ssDNA-tail (total tail length = 79 nts). The ssDNA base compositions tested were (dC_{40}), $d(CT)_{20}$, $d(CA)_{20}$, and $d(AGTC)_{10}$. Base compositions were selected to minimize potential basepairing interactions under our experimental conditions using UNAfold (PrimerQuest program, IDT, Coralville, IA; retrieved 12 December, 2012; http://www.idtdna.com/Scitools). Because our substrates were constrained to have stretches of dT flanking the variable ssDNA region as mentioned above, we were not able to test a poly dA composition due to basepairing. DNA sequences rich in guanosine were also avoided because these resulted

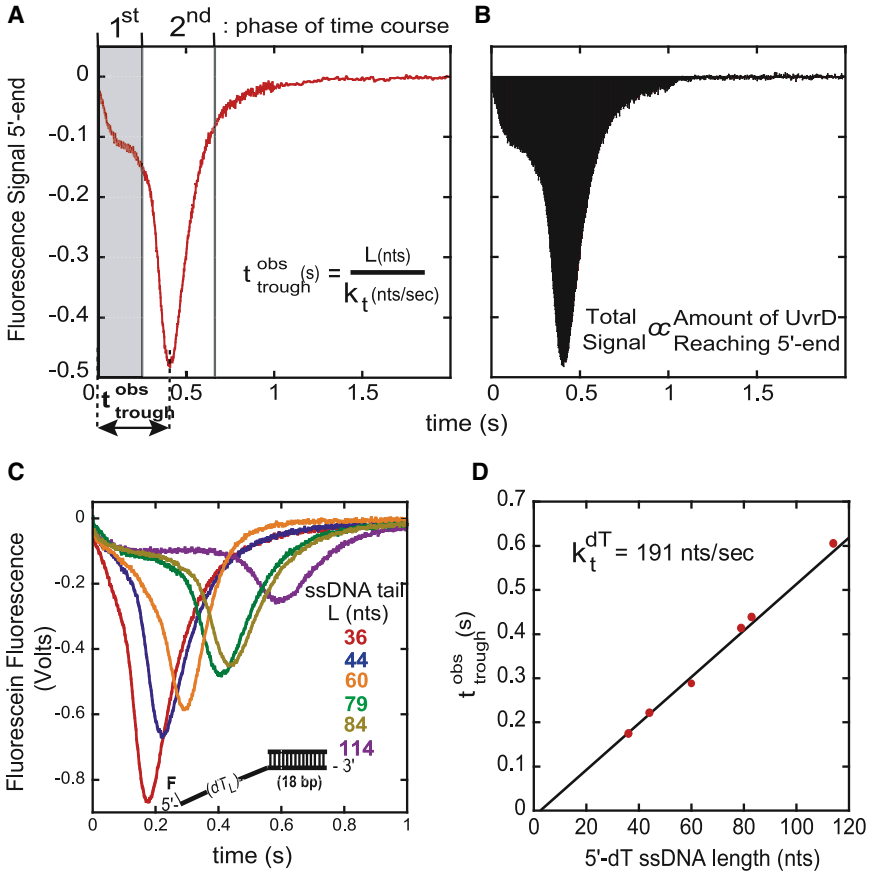

FIGURE 3 Experimental approach for measuring UvrD monomer translocation rate and relative processivity on ssDNA with different base composition. (*A*) Representative time course of UvrD translocation on 5′-ss/dsDNA partial duplex is given. The first phase of the time course reflects translocation to the 5′ end by UvrD initially bound randomly to the ssDNA tail. The second phase reflects translocation to the 5′ end by UvrD that is initially bound at the ss/ds DNA junction. The time-to-trough is related to the average translocation rate. (*B*) A relative translocation processivity is determined from the total area of the fluorescence signal change relative to the control. (*C*) Given here are UvrD monomer translocation time courses on 5′-F-dT_L-DP_{18} partial duplex substrates of variable ssDNA tail lengths, *L*. (*D*) Shown here is a plot of the time-to-trough as a function of ssDNA tail length. The inverse of the slope gives the translocation rate along $(dT)_L$ ssDNA (191 nts/s). To see this figure in color, go online.

in substrates that slowly aggregated over time under the experimental solution conditions.

UvrD (25 nM, postmix) was preincubated with a two-fold molar excess DNA substrate (50 nM, postmix), ensuring that no more than a UvrD monomer is bound to any DNA substrate, in T_{20} buffer at 25°C (18). The UvrD:DNA complex was then mixed rapidly with ATP, $MgCl_2$, and heparin (0.5 mM, 2.0 mM, and 4 mg/mL, respectively) in a stopped-flow instrument to initiate translocation. Heparin was used as a trap for free UvrD, thus preventing free UvrD from reinitiating translocation (9,10). Fig. 4 *A* shows the time courses of UvrD monomer arrival at the 5′-end of the 5′-ss/dsDNA substrates containing different ssDNA base compositions compared to the control substrate, 5′-F-dT_{79}-DP_{18}. The translocation time courses for the DNA with different base composition show a shift in the fluorescence signal minimum to longer times, suggesting that translocation rates become slower as the base composition is changed ($dT > d(CT)_{20} > dC_{40} > d(AGTC)_{10}$). The amplitude of the initial phase of the time course also changes with different base compositions (increasing for dC and decreasing for d(AGTC)), suggesting different affinities for UvrD binding to different ssDNA base compositions.

Comparison of the areas of the translocation signal indicates a decrease in the amount of UvrD that reaches the 5′-end of ssDNA as the purine composition increases, suggesting translocation along purines reduces translocation processivity (Fig. 4 *B*). To confirm that the shifts in trough time are due to the differences in base composition, we changed the length of the variable region of the ssDNA (10–40 nts). Fig. 4, *C* and *D*, shows translocation time courses obtained on 5′-ss/dsDNA substrates with dC and d(CA), respectively. As the length of the ssDNA with different base composition increases, the time to trough shifts to longer times. The average time to transverse the variable base composition region (t_{dvr}) was determined from the trough time as described in Materials and Methods and plotted as a function of the length of the DNA with variable base composition. Plots of t_{dvr}(s) versus length of the variable base composition (Fig. 4 *E*) are linear, yielding translocation rate estimates of 141 ± 3 and 135 ± 1 nts/s for the dC and d(CA) sequences, respectively. The translocation rate over a given sequence can also be estimated using time courses for a single DNA length as in Fig. 4 *A* (see Materials and Methods). The translocation rates determined using DNA of a single length are in good agreement with the translocation rate determined using a series of DNA of different lengths. Table 1 summarizes the results. The UvrD monomer translocation rate is highest along dT ssDNA. The translocation rate decreases to 141 ± 3 nts/s along deoxycytidylates, whereas translocation rates along the dinucleotide repeat d(CT) decrease only slightly to

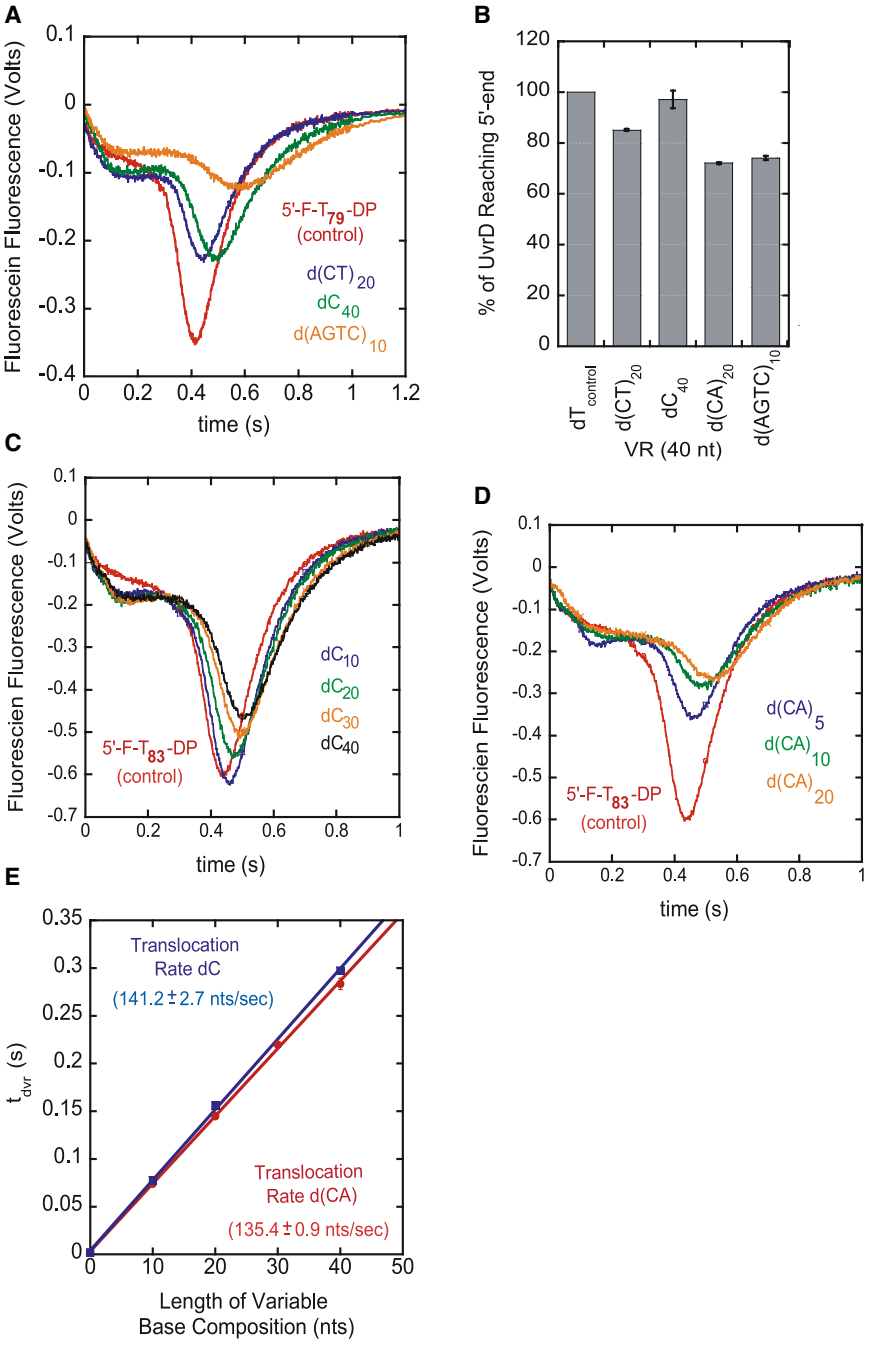

FIGURE 4 UvrD monomer translocation rate is affected by ssDNA base composition. (*A*) Given here are time courses of UvrD (25 nM) monomer translocation along 5′-F-ss/dsDNA substrates (50 nM) with a total ssDNA tail length of 79 nts, but containing 40 nt inserts of varying ssDNA base composition as indicated (T20 buffer, 0.5 mM ATP, 2.0 mM $MgCl_2$, and 4 mg/mL heparin at 25°C). Shown here is the control translocation time course obtained with 5′-F-dT_{79}-DP_{18} (*red*). (*B*) Given here is the fraction of UvrD reaching the 5′-end of the DNA as determined from the total area under the translocation time course from time courses in (*A*), (*C*), and (*D*). Error bars represent the SD of three experiments. (*C* and *D*) Given here are time courses for UvrD monomer translocation along 5′-F-ss/dsDNA substrates with varying lengths of dC and dCdA repeats, respectively. The total ssDNA tail length is 83 nts. Shown here is the control translocation time course obtained with 5′-F-dT_{83}-DP_{18}. (*E*) Given here is the translocation time (t_{dvr}) along dC (*blue*) or dCdA (*red*) ssDNA as a function of the length of the ssDNA of variable base composition. The translocation time, t_{dvr}, is determined from t_{trough}^{obs} as described in Materials and Methods. The inverse of the slope of the linear fit yields the translocation rate along dC and dCdA repeats. To see this figure in color, go online.

169 nts/s. The incorporation of deoxyadenosine and deoxyguanosine within the tetra-nucleotide repeat (dAGTC) further decreases the translocation rate to 107 nts/s.

A single abasic site or polyethylene glycol spacer in the ssDNA backbone increases UvrD dissociation from ssDNA during translocation

A crystal structure of UvrD in complex with a 3′-ss/dsDNA junction (7) shows stacking interactions between the ssDNA bases and aromatic residues of the protein in the ssDNA binding cleft, suggesting UvrD interaction with the ssDNA bases may be important for translocation. Similar interactions were also observed in crystal structures of PcrA bound to a 3′-ss/dsDNA junction (53), and *E. coli* Rep bound to ssDNA (54). To investigate the effects of such stacking interactions on ssDNA translocation of UvrD, we examined ssDNA containing abasic sites. For this, we designed 5′-ss/dsDNA partial duplex substrates with a 5′-$(dT)_{60}$ ssDNA tail labeled with fluorescein at the 5′-end with a variable number of abasic sites (1, 3, or 5 nts) inserted in the middle of the $(dT)_{60}$ as shown in Fig. 5 *A*.

TABLE 1 Effect of ssDNA Base Composition on UvrD Monomer Translocation Rate

Variable Region Composition	Translocation Rate (nts/s) Determined with Single Length (40 nts)	Translocation Rate (nts/s) Determined with Multiple Lengths (10–40 nts)
dT	190	191 ± 2.0
d(CT)	169	N.D.
dC	138	141 ± 3.0
d(CA)	135	135 ± 1.0
d(AGTC)	107	ND

Error represents the SD of three measurements. ND, not determined; nts, nucleotides.

Fig. 5 *B* shows the translocation time courses for three control substrates, (5′-F-dT_{60}-DP_{18}), 5′-F-dT_{30}, and 5′-F-dT_{30}-AB_1-dT_{29}, along with 5′-ss/dsDNA partial duplex substrates containing 1, 3, and 5 consecutive abasic sites. As with 5′-ss/dsDNA partial duplex substrates, the partial duplex substrates containing the abasic sites show two phases. The first phase shows a decrease in fluorescence and is similar to the time-course profile for UvrD translocation along the entire ssDNA tail, rather than just the dT_{30} region upstream of the abasic site (compare 5′-F-dT_{30} and 5′-F-dT_{30}-AB_1-dT_{29} in Fig. 5 *B*). We note that in Fig. 5, *B* and *E*, the fluorescence time course for the dT_{30}-only DNA has been rescaled to be similar in magnitude to the initial phase of the partial duplex substrates. This was done because more UvrD is initially bound to the dT_{30}-only substrate as compared to the dT_{30} region of the partial duplex substrate, and because UvrD has higher affinity for the ss/dsDNA junction (18). The second phase shows a larger decrease in fluorescence and corresponds to the arrival at the 5′−end of UvrD that was initially bound at the ss/dsDNA junction. The time-to-trough for the abasic substrates and the control partial duplex substrate are very similar, with only a slight shift to earlier times for the substrates containing three and five abasic sites. This suggests that the translocation rate for UvrD monomers is not greatly affected by the presence of the abasic sites; however, the amplitude of the second phase decreases as the number of abasic sites increases, indicating less UvrD is able to traverse the abasic sites and reach the 5′-end.

Analysis of the translocation signal suggests that ∼80% of UvrD reaches the 5′-end when there is a single abasic site but this decreases to 40 and 30% when there is a stretch of three or five abasic sites, respectively (Fig. 5 *F*). We next monitored UvrD dissociation kinetics during translocation to see if the decrease in amplitude is due to increased UvrD dissociation from the ssDNA at the abasic sites. UvrD dissociation from the ssDNA during translocation was monitored by the increase in intrinsic tryptophan fluorescence of UvrD (Fig. 5 *C*). Indeed, a faster dissociation phase is observed for the DNA containing the abasic sites and this increases as the number of abasic sites increase. Thus, UvrD has a higher probability of dissociating from the ssDNA when it encounters an abasic site under our solution conditions.

Because some fraction of UvrD was able to translocate past the abasic sites, we also examined the effect of incorporating a polyethylene glycol (PEG) spacer (55). PEG spacers are uncharged and lack a phosphodiester backbone structure. Three PEG spacers have the equivalent contour length of ∼1.5 nts (55,56). We tested UvrD translocation on four partial duplex substrates containing PEG spacers with contour length equivalents of 1.5 nts (PEG3), 3 nts (PEG6), 4.5 nts (PEG9), and 15 nts (PEG30). Fig. 5 *D* shows that the amount of UvrD that reaches the 5′-end decreases as the PEG spacer length increases. None of the UvrD is able to bypass the longest PEG insert (PEG30), with a contour length equivalent to 15 nts. The only UvrD that reaches the 5′-end on this DNA substrate is the UvrD that was initially bound to the dT_{30} region upstream of the PEG spacers as the time course for this substrate overlays exactly with the time course for dT_{30}, scaled to match the fluorescence of the PEG30 substrate (Fig. 5 *D*). This indicates that UvrD is not able to translocate past stretches of PEG greater than its contact size on the DNA (∼8–10 nts (5)). However, a surprising amount of UvrD is able to bypass the shorter PEG spacers (Fig. 5 *F*).

The UvrD monomer dissociation time courses from the PEG spacer substrates (Fig. 5 *E*) also show a faster dissociation phase compared to the control substrate and the abasic site substrates, suggesting a faster UvrD dissociation rate upon encountering the PEG spacers. Comparisons of the translocation time courses obtained with the abasic site DNA substrates (Fig. 5, *B* and *C*) and PEG spacer substrates (Fig. 5, *D* and *E*) suggest that the PEG spacers lower translocation processivity more than the abasic sites, especially for longer stretches of PEG (compare five abasic sites to PEG 4.5 nt equivalent; Fig. 5 *F*).

DISCUSSION

We show here that UvrD monomer translocation rate depends on the ssDNA base composition, even in the absence of any predicted basepairing within the nucleic acid. Translocation is faster on ssDNA-containing pyrimidines and slower on ssDNA-containing purines. This trend is very different than that reported for PcrA translocation, which was concluded to be fastest along dC followed by dA ∼ dT using a different analysis of a fluorescence assay monitoring dissociation of PcrA during translocation (57). However, the method of analysis used in that study has been shown to overestimate the rates of ssDNA translocation (51). Furthermore, those authors note that their analysis may be complicated by nonuniform binding of PcrA to the DNA. We avoided such complications by utilizing ssDNA substrates with a 5′-ssDNA tail labeled at the 5′-end with fluorescein and a DNA partial duplex at the opposite end. UvrD monomers show a preference for binding to a ss/ds DNA junction, although UvrD does not exclusively bind to the junction (18). However, the resulting time courses can be readily analyzed by measuring the change in the time-to-trough as a function of ssDNA length to obtain

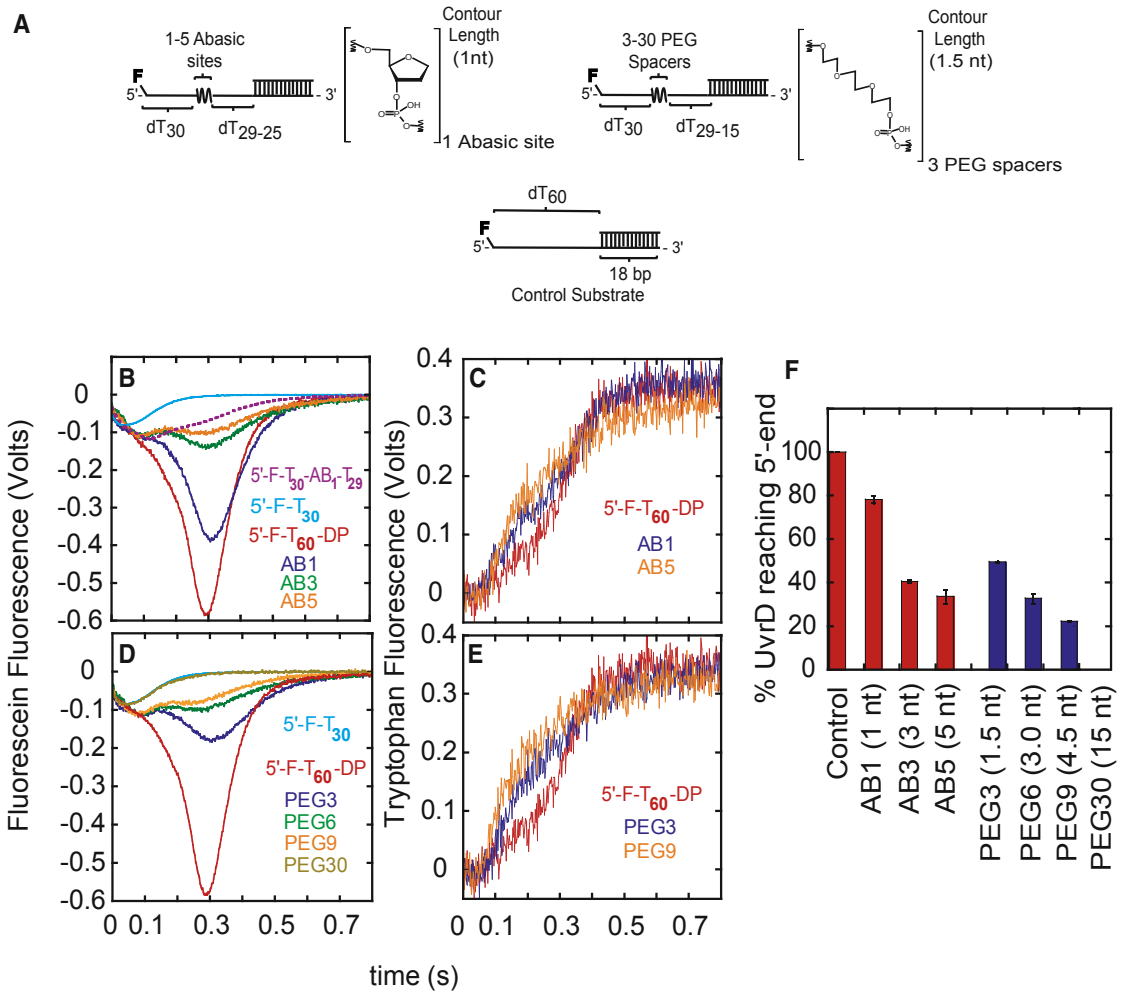

FIGURE 5 Insertion of abasic sites or PEG spacers increases the probability of UvrD dissociation from the ssDNA during translocation. (*A*) Schematic of 5′-F-ss/dsDNA substrates with abasic sites $(AB)_N$ ($N = 1$, 3, or 5) or PEG spacers is given. The total ssDNA tail length is constant at 60 nts. (*B*) Given here are translocation time courses monitoring arrival of UvrD at the 5′-end of the ssDNA on 5′-F-ss/dsDNA substrates with abasic sites ($N = 1$, 3, and 5 sites) and control substrates. (*C*) Given here are UvrD dissociation time courses during translocation on 5′-F-ss/dsDNA substrates with abasic sites ($N = 1$, 3, and 5 sites) and control substrates. (*D*) Given here are translocation time courses monitoring the arrival of UvrD at the 5′-end of the ssDNA on 5′-F-ss/dsDNA substrates with PEG spacers (1.5, 3, 4.5, and 15 nts equivalents) and control substrates. (*E*) Given here are UvrD dissociation time courses during translocation on 5′-F-ss/dsDNA substrates with PEG spacers (1.5, 3, 4.5, and 15 nts equivalents) and control substrates. (*F*) Shown here is the percentage of UvrD initially bound at the ss/ds DNA junction that reaches the 5′-end during translocation along ssDNA containing either abasic sites or PEG spacers. Error bars represent SD of three experiments. To see this figure in color, go online.

the translocation rate without requiring information about the translocation processivity (46). The base composition also affects UvrD translocation processivity, such that incorporation of purines reduces processivity (Fig. 4 *B*). Significantly, the incorporation of an abasic site increases the probability of UvrD dissociation from the ssDNA. Hence the nucleic acid bases have a direct impact on translocation of UvrD and possibly other UvrD-like SF1 DNA helicases.

Mechanistic implications for SF1 DNA helicase ssDNA translocation

In crystal structures of UvrD (7), Rep (54), and PcrA (53) in complex with DNA, the ssDNA binding cleft along the top of the 2A and 1A subdomains forms two pockets, each of which bind two consecutive nucleotides of the ssDNA. Between the two pockets, a portion of the 1A subdomain protrudes upward, causing one nucleotide residue to be flipped out of plane with the ssDNA residues bound in the pockets (7). These observations for PcrA, which are similar to those for UvrD (7), led to the proposal of an inchworm translocation mechanism where the relative movements of the 1A and 2A subdomains, modulated by ATP binding and hydrolysis, are coordinated with stacking interactions between aromatic side chains and the ssDNA bases (53,58).

Because these proteins contact the aromatic bases of the ssDNA, it was hypothesized that nucleotide base composition would have a larger impact on translocation than

changes to the sugar-phosphate backbone (59). Our results show that the UvrD monomer translocation rate is affected by base composition, consistent with this hypothesis. Furthermore, our results with substrates containing abasic sites or PEG spacers reveal that the organic base itself affects translocation processivity, because removal of the organic base results in an increased UvrD dissociation rate. We note that although heparin can actively displace UvrD from ssDNA during translocation, this does not affect the translocation rate, but only the apparent processivity (9).

Interestingly, the base-dependent reduction in translocation rate follows the stacking propensity for nucleotide bases, such that the fastest translocation is observed on stretches of dT (190 nts/s), which shows little stacking, and the slowest translocation is observed on ssDNA-containing purines (dCA = 135 nts/s, dAGTC = 107 nts/s), which favor base stacking (60–67). This observation suggests that translocation rate is slower when stacking interactions need to be disrupted. Interestingly, a recent single molecule study of UvrD monomer translocation on a mixed sequence ssDNA from λ-DNA reported a translocation rate similar to that observed in ensemble studies with poly(dT) (11). In the single molecule study, the ssDNA was held at an ∼10 pN force that is sufficient to disrupt base-stacking interactions (11,68). Moreover, as the force was reduced a slower translocation rate was observed (11), suggesting either base-stacking and or internal basepair formation was slowing translocation. In another single molecule study using magnetic tweezers (69), large applied forces to the DNA (>30 pN) facilitated DNA unwinding by UvrD, resulting in higher DNA unwinding processivity and an unwinding rate similar to the ssDNA translocation rate measured on poly(dT) (9,10,19). Such forces can disrupt base-stacking interactions, obscuring any potential base-stacking effect on translocation. In light of our observations, one needs to consider the effect of applied force and other conditions that affect base stacking on the mechanisms of nucleic acid motors.

Mechanistically, ssDNA base stacking may stabilize interactions between UvrD amino acid side chains and the ssDNA, possibly hindering flipping of the nucleotide between the two pockets observed in the crystal structure and thus slowing translocation. Alternatively, base stacking might result in less flexibility of the ssDNA backbone that may hinder translocation. Indeed, DNA substrates containing a torsionally constrained ssDNA backbone on the tracking strand have been shown to inhibit DNA unwinding by PcrA, suggesting backbone flexibility facilitates translocation (70).

Studies of ssDNA/ssRNA translocation of the SF2 DNA/RNA helicase NS3h from Hepatitis C virus have suggested that higher affinity of the enzyme for the nucleic acid results in slower translocation rates (45). Our work with UvrD reveals that ssDNA base composition affects translocation along the ssDNA, likely as a result of effects on base stacking. Regardless of origin, such effects of base composition need to be considered when comparing rates of ssDNA translocation with rates of DNA unwinding.

SUPPORTING MATERIAL

Supporting Materials and Methods and one table are available at http://www.biophysj.org/biophysj/supplemental/S0006-3495(17)30916-5.

AUTHOR CONTRIBUTIONS

E.J.T. and T.M.L. designed the experiments and wrote the article. E.J.T. performed the experiments and analyzed the data.

ACKNOWLEDGMENTS

We thank Chris Fischer for conducting initial experiments with oligo dC substrates.

This research was supported in part by National Institutes of Health (NIH) grant GM45948 to T.M.L.

SUPPORTING CITATIONS

References (71–73) appear in the Supporting Material.

REFERENCES

1. Matson, S. W. 1986. *Escherichia coli* helicase II (urvD gene product) translocates unidirectionally in a 3′ to 5′ direction. *J. Biol. Chem.* 261:10169–10175.
2. Runyon, G. T., D. G. Bear, and T. M. Lohman. 1990. *Escherichia coli* helicase II (UvrD) protein initiates DNA unwinding at nicks and blunt ends. *Proc. Natl. Acad. Sci. USA.* 87:6383–6387.
3. Runyon, G. T., and T. M. Lohman. 1989. *Escherichia coli* helicase II (uvrD) protein can completely unwind fully duplex linear and nicked circular DNA. *J. Biol. Chem.* 264:17502–17512.
4. Runyon, G. T., and T. M. Lohman. 1993. Kinetics of *Escherichia coli* helicase II-catalyzed unwinding of fully duplex and nicked circular DNA. *Biochemistry.* 32:4128–4138.
5. Runyon, G. T., I. Wong, and T. M. Lohman. 1993. Overexpression, purification, DNA binding, and dimerization of the *Escherichia coli* uvrD gene product (helicase II). *Biochemistry.* 32:602–612.
6. Maluf, N. K., C. J. Fischer, and T. M. Lohman. 2003. A dimer of *Escherichia coli* UvrD is the active form of the helicase in vitro. *J. Mol. Biol.* 325:913–935.
7. Lee, J. Y., and W. Yang. 2006. UvrD helicase unwinds DNA one base pair at a time by a two-part power stroke. *Cell.* 127:1349–1360.
8. Jia, H., S. Korolev, …, T. M. Lohman. 2011. Rotations of the 2B subdomain of *E. coli* UvrD helicase/translocase coupled to nucleotide and DNA binding. *J. Mol. Biol.* 411:633–648.
9. Fischer, C. J., N. K. Maluf, and T. M. Lohman. 2004. Mechanism of ATP-dependent translocation of *E. coli* UvrD monomers along single-stranded DNA. *J. Mol. Biol.* 344:1287–1309.
10. Tomko, E. J., C. J. Fischer, …, T. M. Lohman. 2007. A nonuniform stepping mechanism for *E. coli* UvrD monomer translocation along single-stranded DNA. *Mol. Cell.* 26:335–347.
11. Lee, K. S., H. Balci, …, T. Ha. 2013. Direct imaging of single UvrD helicase dynamics on long single-stranded DNA. *Nat. Commun.* 4:1878.
12. Iyer, R. R., A. Pluciennik, …, P. L. Modrich. 2006. DNA mismatch repair: functions and mechanisms. *Chem. Rev.* 106:302–323.

13. Sancar, A. 1996. DNA excision repair. *Annu. Rev. Biochem.* 65:43–81.
14. Atkinson, J., and P. McGlynn. 2009. Replication fork reversal and the maintenance of genome stability. *Nucleic Acids Res.* 37:3475–3492.
15. Heller, R. C., and K. J. Marians. 2007. Non-replicative helicases at the replication fork. *DNA Repair (Amst.).* 6:945–952.
16. Florés, M. J., N. Sanchez, and B. Michel. 2005. A fork-clearing role for UvrD. *Mol. Microbiol.* 57:1664–1675.
17. Bruand, C., and S. D. Ehrlich. 2000. UvrD-dependent replication of rolling-circle plasmids in *Escherichia coli*. *Mol. Microbiol.* 35:204–210.
18. Tomko, E. J., H. Jia, …, T. M. Lohman. 2010. 5′-Single-stranded/duplex DNA junctions are loading sites for *E. coli* UvrD translocase. *EMBO J.* 29:3826–3839.
19. Tomko, E. J., C. J. Fischer, and T. M. Lohman. 2012. Single-stranded DNA translocation of *E. coli* UvrD monomer is tightly coupled to ATP hydrolysis. *J. Mol. Biol.* 418:32–46.
20. Maluf, N. K., J. A. Ali, and T. M. Lohman. 2003. Kinetic mechanism for formation of the active, dimeric UvrD helicase-DNA complex. *J. Biol. Chem.* 278:31930–31940.
21. Comstock, M. J., K. D. Whitley, …, Y. R. Chemla. 2015. Protein structure. Direct observation of structure-function relationship in a nucleic acid-processing enzyme. *Science.* 348:352–354.
22. Sun, B., K. J. Wei, …, X. G. Xi. 2008. Impediment of *E. coli* UvrD by DNA-destabilizing force reveals a strained-inchworm mechanism of DNA unwinding. *EMBO J.* 27:3279–3287.
23. Veaute, X., S. Delmas, …, M. A. Petit. 2005. UvrD helicase, unlike Rep helicase, dismantles RecA nucleoprotein filaments in *Escherichia coli*. *EMBO J.* 24:180–189.
24. Petrova, V., S. H. Chen, …, M. M. Cox. 2015. Active displacement of RecA filaments by UvrD translocase activity. *Nucleic Acids Res.* 43:4133–4149.
25. Sokoloski, J. E., A. G. Kozlov, …, T. M. Lohman. 2016. Chemo-mechanical pushing of proteins along single-stranded DNA. *Proc. Natl. Acad. Sci. USA.* 113:6194–6199.
26. Boubakri, H., A. L. de Septenville, …, B. Michel. 2010. The helicases DinG, Rep and UvrD cooperate to promote replication across transcription units in vivo. *EMBO J.* 29:145–157.
27. McGlynn, P., N. J. Savery, and M. S. Dillingham. 2012. The conflict between DNA replication and transcription. *Mol. Microbiol.* 85:12–20.
28. Epshtein, V., V. Kamarthapu, …, E. Nudler. 2014. UvrD facilitates DNA repair by pulling RNA polymerase backwards. *Nature.* 505:372–377.
29. Lohman, T. M. 1992. *Escherichia coli* DNA helicases: mechanisms of DNA unwinding. *Mol. Microbiol.* 6:5–14.
30. Lohman, T. M., and K. P. Bjornson. 1996. Mechanisms of helicase-catalyzed DNA unwinding. *Annu. Rev. Biochem.* 65:169–214.
31. Manosas, M., X. G. Xi, …, V. Croquette. 2010. Active and passive mechanisms of helicases. *Nucleic Acids Res.* 38:5518–5526.
32. Betterton, M. D., and F. Jülicher. 2005. Opening of nucleic-acid double strands by helicases: active versus passive opening. *Phys. Rev. E Stat. Nonlin. Soft Matter Phys.* 71:011904.
33. Xie, F., C. G. Wu, …, T. M. Lohman. 2013. Asymmetric regulation of bipolar single-stranded DNA translocation by the two motors within *Escherichia coli* RecBCD helicase. *J. Biol. Chem.* 288:1055–1064.
34. Lucius, A. L., C. J. Wong, and T. M. Lohman. 2004. Fluorescence stopped-flow studies of single turnover kinetics of *E. coli* RecBCD helicase-catalyzed DNA unwinding. *J. Mol. Biol.* 339:731–750.
35. Wu, C. G., and T. M. Lohman. 2008. Influence of DNA end structure on the mechanism of initiation of DNA unwinding by the *Escherichia coli* RecBCD and RecBC helicases. *J. Mol. Biol.* 382:312–326.
36. Wu, C. G., C. Bradford, and T. M. Lohman. 2010. *Escherichia coli* RecBC helicase has two translocase activities controlled by a single ATPase motor. *Nat. Struct. Mol. Biol.* 17:1210–1217.
37. Niedziela-Majka, A., M. A. Chesnik, …, T. M. Lohman. 2007. *Bacillus stearothermophilus* PcrA monomer is a single-stranded DNA translocase but not a processive helicase in vitro. *J. Biol. Chem.* 282:27076–27085.
38. Brendza, K. M., W. Cheng, …, T. M. Lohman. 2005. Autoinhibition of *Escherichia coli* Rep monomer helicase activity by its 2B subdomain. *Proc. Natl. Acad. Sci. USA.* 102:10076–10081.
39. Byrd, A. K., D. L. Matlock, …, K. D. Raney. 2012. Dda helicase tightly couples translocation on single-stranded DNA to unwinding of duplex DNA: Dda is an optimally active helicase. *J. Mol. Biol.* 420:141–154.
40. Lohman, T. M., E. J. Tomko, and C. G. Wu. 2008. Non-hexameric DNA helicases and translocases: mechanisms and regulation. *Nat. Rev. Mol. Cell Biol.* 9:391–401.
41. Young, M. C., D. E. Schultz, …, P. H. von Hippel. 1994. Kinetic parameters of the translocation of bacteriophage T4 gene 41 protein helicase on single-stranded DNA. *J. Mol. Biol.* 235:1447–1458.
42. Arai, N., K. Arai, and A. Kornberg. 1981. Complexes of *Rep* protein with ATP and DNA as a basis for helicase action. *J. Biol. Chem.* 256:5287–5293.
43. Dillingham, M. S., D. B. Wigley, and M. R. Webb. 2000. Demonstration of unidirectional single-stranded DNA translocation by PcrA helicase: measurement of step size and translocation speed. *Biochemistry.* 39:205–212.
44. Slatter, A. F., C. D. Thomas, and M. R. Webb. 2009. PcrA helicase tightly couples ATP hydrolysis to unwinding double-stranded DNA, modulated by the initiator protein for plasmid replication, RepD. *Biochemistry.* 48:6326–6334.
45. Khaki, A. R., C. Field, …, C. J. Fischer. 2010. The macroscopic rate of nucleic acid translocation by hepatitis C virus helicase NS3h is dependent on both sugar and base moieties. *J. Mol. Biol.* 400:354–378.
46. Tomko, E. J., C. J. Fischer, and T. M. Lohman. 2010. Ensemble methods for monitoring enzyme translocation along single stranded nucleic acids. *Methods.* 51:269–276.
47. Dillingham, M. S., D. B. Wigley, and M. R. Webb. 2002. Direct measurement of single-stranded DNA translocation by PcrA helicase using the fluorescent base analogue 2-aminopurine. *Biochemistry.* 41:643–651.
48. Fischer, C. J., E. J. Tomko, …, T. M. Lohman. 2012. Fluorescence methods to study DNA translocation and unwinding kinetics by nucleic acid motors. *Methods Mol. Biol.* 875:85–104.
49. Wu, C. G., F. Xie, and T. M. Lohman. 2012. The primary and secondary translocase activities within *E. coli* RecBC helicase are tightly coupled to ATP hydrolysis by the RecB motor. *J. Mol. Biol.* 423:303–314.
50. Galletto, R., and E. J. Tomko. 2013. Translocation of *Saccharomyces cerevisiae* Pif1 helicase monomers on single-stranded DNA. *Nucleic Acids Res.* 41:4613–4627.
51. Fischer, C. J., and T. M. Lohman. 2004. ATP-dependent translocation of proteins along single-stranded DNA: models and methods of analysis of pre-steady state kinetics. *J. Mol. Biol.* 344:1265–1286.
52. Fischer, C. J., L. Wooten, …, T. M. Lohman. 2010. Kinetics of motor protein translocation on single-stranded DNA. *Methods Mol. Biol.* 587:45–56.
53. Velankar, S. S., P. Soultanas, …, D. B. Wigley. 1999. Crystal structures of complexes of PcrA DNA helicase with a DNA substrate indicate an inchworm mechanism. *Cell.* 97:75–84.
54. Korolev, S., J. Hsieh, …, G. Waksman. 1997. Major domain swiveling revealed by the crystal structures of complexes of *E. coli* Rep helicase bound to single-stranded DNA and ADP. *Cell.* 90:635–647.
55. Amaratunga, M., and T. M. Lohman. 1993. *Escherichia coli* rep helicase unwinds DNA by an active mechanism. *Biochemistry.* 32:6815–6820.
56. Williams, D. J., and K. B. Hall. 1996. Thermodynamic comparison of the salt dependence of natural RNA hairpins and RNA hairpins with non-nucleotide spacers. *Biochemistry.* 35:14665–14670.
57. Chisty, L. T., C. P. Toseland, …, M. R. Webb. 2013. Monomeric PcrA helicase processively unwinds plasmid lengths of DNA in the presence of the initiator protein RepD. *Nucleic Acids Res.* 41:5010–5023.

58. Soultanas, P., and D. B. Wigley. 2000. DNA helicases: 'inching forward'. *Curr. Opin. Struct. Biol.* 10:124–128.

59. Saikrishnan, K., B. Powell, …, D. B. Wigley. 2009. Mechanistic basis of 5′-3′ translocation in SF1B helicases. *Cell.* 137:849–859.

60. Riley, M., and B. Maling. 1966. Physical and chemical characterization of two- and three-stranded adenine-thymine and adenine-uracil homopolymer complexes. *J. Mol. Biol.* 20:359–389.

61. Luzzati, V., A. Mathis, …, J. Witz. 1964. Structure transitions observed in DNA and poly A in solution as function of temperature and pH. *J. Mol. Biol.* 10:28–41.

62. Leng, M., and G. Felsenfeld. 1966. A study of polyadenylic acid at neutral pH. *J. Mol. Biol.* 15:455–466.

63. Poland, D., J. N. Vournakis, and H. A. Scheraga. 1966. Cooperative interactions in single-strand oligomers of adenylic acid. *Biopolymers.* 4:223–235.

64. Vournakis, J. N., D. Poland, and H. A. Scheraga. 1967. Anti-cooperative interactions in single-strand oligomers of deoxyriboadenylic acid. *Biopolymers.* 5:403–422.

65. Ts'o, P. O. P., S. A. Rapaport, and F. J. Bollum. 1966. A comparative study of polydeoxyribonucleotides and polyribonucleotides by optical rotatory dispersion. *Biochemistry.* 5:4153–4170.

66. Ferrari, M. E., and T. M. Lohman. 1994. Apparent heat capacity change accompanying a nonspecific protein-DNA interaction. *Escherichia coli* SSB tetramer binding to oligodeoxyadenylates. *Biochemistry.* 33:12896–12910.

67. Kozlov, A. G., and T. M. Lohman. 1999. Adenine base unstacking dominates the observed enthalpy and heat capacity changes for the *Escherichia coli* SSB tetramer binding to single-stranded oligoadenylates. *Biochemistry.* 38:7388–7397.

68. McIntosh, D. B., G. Duggan, …, O. A. Saleh. 2014. Sequence-dependent elasticity and electrostatics of single-stranded DNA: signatures of base-stacking. *Biophys. J.* 106:659–666.

69. Dessinges, M. N., T. Lionnet, …, V. Croquette. 2004. Single-molecule assay reveals strand switching and enhanced processivity of UvrD. *Proc. Natl. Acad. Sci. USA.* 101:6439–6444.

70. Bertram, R. D., C. J. Hayes, and P. Soultanas. 2002. Vinyl phosphonate internucleotide linkages inhibit the activity of PcrA DNA helicase. *Biochemistry.* 41:7725–7731.

71. Wolf, A. V., M. G. Brown, and P. G. Prentiss. 1974. Concentrative properties of aqueous solutions: conversion tables. *In* CRC Handbook of Chemical and Physical Data. R. C. Weast, ed. CRC Press, Cleveland, Ohio, D-209.

72. Mascotti, D. P., and T. M. Lohman. 1995. Thermodynamics of charged oligopeptide-heparin interactions. *Biochemistry.* 34:2908–2915.

73. Gray, D. M., S. H. Hung, and K. H. Johnson. 1995. Absorption and circular dichroism spectroscopy of nucleic acid duplexes and triplexes. *Methods Enzymol.* 246:19–34.